GEOPHYSICS, VOL. 66, NO. 5 (SEPTEMBER-OCTOBER 2001); P. 1622–1640, 18 FIGS.

Y2K Review Article

Seismic migration problems and solutions

Samuel H. Gray*, John Etgen‡, Joe Dellinger‡, and Dan Whitmore**

ABSTRACT

Historically, seismic migration has been the practice (science, technology, and craft) of collapsing diffraction events on unmigrated records to points, thereby moving ("migrating") reflection events to their proper locations, creating a true image of structures within the earth. Over the years, the scope of migration has broadened. What began as a structural imaging tool is evolving into a tool for velocity estimation and attribute analysis, making detailed use of the amplitude and phase information in the migrated image. With its expanded scope, migration has moved from the final step of the seismic acquisition and processing flow to a more central one, with links to both the processes preceding and following it.

In this paper, we describe the mechanics of migration (the algorithms) as well as some of the problems related to it, such as algorithmic accuracy and efficiency, and velocity estimation. We also describe its relationship with other processes, such as seismic modeling. Our approach is tutorial; we avoid presenting the finest details of either the migration algorithms themselves or the problems to which migration is applied. Rather, we focus on presenting the problems themselves, in the hope that most geophysicists will be able to gain an appreciation of where this imaging method fits in the larger problem of searching for hydrocarbons.

INTRODUCTION AND HISTORICAL PERSPECTIVE

Seismic migration is a wave-equation-based process that removes distortions from reflection records by moving events to their correct spatial locations and by collapsing energy from diffractions back to their scattering points. Today, migration is a central step in the seismic data processing flow. It represents the culmination of "standard" processing, and it provides input for several relatively exotic nonstandard processes. Migration has not always occupied this central location in the flow; until a decade ago, migration was often an optional final processing step. After such steps as scaling, deconvolution, statics and velocity analysis, the application of dip-moveout (DMO) corrections and common-midpoint (CMP) stacking, the final stack would be migrated to provide a structural image for interpretation. In cases where diffraction events on the unmigrated stack obscured subtle targets such as pinch-outs and reef edges, migration might be performed for stratigraphic imaging purposes as well. In contrast, present-day seismic data are almost always migrated, usually before stack, and interpreting migrated data often involves further detailed analysis of the migrated amplitudes or other attributes.

Migration actually predates most of seismic processing. Implemented as early as the 1920s as a graphical method, migration had several predigital incarnations, all of which embodied the kinematic principles of the diffraction stack and, ultimately, of Kirchhoff migration. Gardner (1985) presents much of the early history of the subject with several papers describing mechanical, as opposed to digital, migration. With the development of the CMP stack (Mayne, 1962) and the application of digital signal processing techniques to seismic data in the 1960s, including digital diffraction stacks (Schneider, 1971), the stage was set for the first wave-equation-based digital migration methods. These came from work in the early 1970s by Jon Claerbout and his students in the Stanford Exploration Project, who derived migration as a finite-difference solution of an approximate wave equation (Claerbout and Doherty, 1972). Kirchhoff wave-equation migration (Schneider, 1978) and frequency-wavenumber

Manuscript received by the Editor September 26, 2000; revised manuscript received March 14, 2001.
*Veritas DGC Ltd., 715 5th Avenue SW, Calgary, Alberta T2P5A2, Canada. E-mail: sam_gray@veritasdgc.com.
‡BP Amoco WL4, Room 1019, 200 Westlake Park Boulevard, Houston, Texas 77079. E-mail: jetgen@amoco.com; dellinja@bp.com.
**Phillips Petroleum Co., 560 Plaza Office Building, Bartlesville, Oklahoma 74004. E-mail: ndwhitm@ppco.com.
© 2001 Society of Exploration Geophysicists. All rights reserved.

migrations (Gazdag, 1978; Stolt, 1978) appeared shortly thereafter. All these methods appeared first as time migrations; then, as the need for improved accuracy in the presence of lateral velocity variations was recognized, some of them were recast within a few years as depth migrations. At about the same time, reverse-time migration appeared (Baysal et al., 1983; McMechan, 1983; Whitmore, 1983). Based on the exact wave equation, not an approximation, this method propagates the recorded wavefield backwards through an interval velocity model of the earth and is, therefore, inherently a depth-migration method. The last 20 years have seen extensions of these methods to three dimensions and to prestack migration, and ever-greater refinements to their efficiency and accuracy.

Migration was one of the earliest seismic imaging tools, but the very earliest was simply the display of single-fold analog seismic records. These records, full of diffracted energy and random noise, still gave a rendition of the earth's subsurface. Mechanical migrations removed the structural distortions present on early seismic records, and the CMP stack reduced the amount of random noise while preserving much of the diffracted energy. CMP-stacked data were used as input for early digital migrations (which were typically limited in their ability to image steep dips) for two reasons. First, the flat-layered earth assumptions used in the normal-moveout (NMO) equations of the CMP stacking process led to the suppression of steep-dip energy on stacked records. Second, the popular finite-difference migration methods were themselves dip limited. The subsequent development of DMO (Judson et al., 1978; Yilmaz, 1979) as a method to improve the dip bandwidth of CMP stacking, and later the discovery that DMO is a component process of prestack migration (Hale, 1984), led to a demand for migration methods with greater steep-dip imaging capability, such as frequency-wavenumber and Kirchhoff methods. With the ability to image steep dips came even more requirements for accuracy in migration, including depth migration, leading to the wide range of migration methods presently available.

Today, a variety of imaging problems exist, related to imaging complex structures or subtle stratigraphy, or to producing estimates of correctly positioned seismic attributes. A similar variety of migration tools is available to solve these problems: in time and depth, in two and three dimensions, and before and after stack. We shall describe in this paper a number of migration-related problems and solutions, as well as other topics that touch on migration, such as the usefulness of seismic modeling in testing and fine-tuning migration algorithms. Any overview of such a large subject will necessarily skip many technical details. Recognizing the limitations of space, we nevertheless hope to present enough of the problems and issues in general terms to hold the attention of readers who are not expert in the field.

Now, geophysicists who plan to migrate their data face a problem that is very different from the problems of a decade ago. Then, geophysicists were likely to be frustrated with the lack of tools available to solve their imaging problems; today, geophysicists who are not migration experts are likely to be confused by the wide range of migration choices available, many of which may be more than adequate for the task. This abundance of choices is not the case with other problems, such as velocity estimation. Whereas estimating imaging velocities for time migration is a routine task, estimating interval velocities for depth migration is a problem that continues to challenge processing and interpreting geophysicists alike. Analyzing migrated amplitudes, say for amplitude-versus-angle (AVA) purposes, is similarly problematic. As important as this application is becoming, along with the analysis of other seismic data attributes, there is still no clear choice of which data-processing flow to use (including the migration algorithm) if true amplitudes in the resulting image are important.

THE ROLE OF SEISMIC MODELING

Seismic modeling and seismic migration are, in some sense, inverses of each other (Santos et al., 2000). Modeling describes the forward process of propagating waves from sources to scatterers to receivers, generating seismic data. Migration attempts to undo the wave-propagation effects to produce an image of the earth. Not surprisingly, seismic migration and seismic modeling have historically had an intimate relationship. Early on, researchers recognized that modeling and migration should be inverse operations, and several migration methods were developed using this fact, most notably reverse-time migration. In this section, we discuss a different aspect of the relationship between modeling and migration, namely the use of numerical modeling to calibrate our migration methods. We focus particularly on the use of finite-difference modeling using the full acoustic or elastic wave equation (Kelly et al., 1976).

Full wave-equation finite-difference (F-D) modeling has no dip limitations and produces all the events associated with the wave equation (e.g., multiple reflections, head waves and, when the elastic wave equation is used, anisotropic effects and mode conversions). F-D modeling is therefore an ideal way to obtain realistic seismic data from a model earth that is precisely known, as opposed to "real" (field) data, which has the troublesome property of coming from the unknown real earth. Although the ultimate goal of migration is to construct images of the earth using "real" data, it is difficult to test the accuracy of migration methods when the desired result, the correct image, is not known.

F-D modeling also has intrinsic advantages over physical-model data, which are recorded over scale earth models using scaled-down sources and receivers, and scaled-down wavelengths and times. Precisely controlling the model geometry at this fine scale is difficult. In consequence, physical models tend to be geometrically simple, consisting of a few homogeneous blocks or layers. If some of these do contain complex internal structure, it comes from the materials used to construct the model, and so is generally unknown in precise detail. Synthetic (computed) data are both as exact and as detailed as we care to make them and, as such, they are clinical, allowing us to study the effects we wish to study.

Kirchhoff migration has always been expensive, and F-D modeling has always been even more expensive. In order to produce accurate synthetic data over propagation ranges of hundreds of wavelengths at seismic frequencies, the modeling algorithms must ensure that artifacts arising from numerical problems such as instability and dispersion are kept under control. Significant progress has been made in reducing these artifacts, but the practicalities of F-D modeling ensure that we will pay handsomely to obtain high-quality synthetic seismic data. Nevertheless, we can take the view that this price is low when it is averaged over hundreds of production runs of a migration code that has been fine-tuned with the help of synthetic data.

The earliest finite-difference models used to test the structural imaging capabilities of migration were 2-D models of

CMP stacked (or more precisely, zero-offset) data. Since zero-offset data do not come from a single wave-equation experiment, it was necessary to contrive an experiment that would mimic the acquisition of a stacked data set. The exploding reflector model (Loewenthal et al., 1976) produced such an experiment. In this model, the reflectors "explode" at time $t = 0$, producing waves which propagate upwards to the earth's surface at one-half the actual velocity. Because the model propagation distance (reflector to surface) is also one-half the actual zero-offset propagation distance (surface to reflector to surface), the modeled zero-offset event times are correct. An exploding-reflector synthetic (computed using the wave equation) thus provides a reasonably faithful representation of a zero-offset seismic section from a known earth. (The exploding reflector model notably fails to include energy that traveled from source to reflector along one path and returned back to the source along a different path.) Migrating an exploding-reflector synthetic produces an image that can be compared with the known model, sometimes successfully but sometimes to the embarrassment of the migration. Figure 1 (from Baysal et al., 1983) shows a successful example of applying migration to data from a realistic model.

This example also illustrates a pitfall to be avoided when migrating model data or, indeed, when using any inverse technique. The method used to migrate this particular data set, reverse-time migration, is seismic modeling in reverse, which is essentially perfect. To obtain model data to test this method, a different—less accurate—modeling method had to be used. Since any other method can only approach the accuracy of using the full wave equation, the model data were less than perfect, and this caused the artifacts that are visible on the migrated image. In general, to validate the inverse of a method, we must use a different, *more accurate*, forward-modeling method to create the data for the test.

One of the best known of all synthetic model data sets is Marmousi (Versteeg and Grau, 1991). Based on a detailed geological 2-D cross section of a real Angola basin, this data set consists of 240 single-cable marine shot records acquired using acoustic F-D modeling, with variations in both acoustic velocity and density. This model was generated by the French Petroleum Institute, and was released to the industry for the purpose of testing migration and velocity estimation techniques.

The Marmousi model is structurally complex, with many very thin layers broken by several major faults and an unconformity surface (Figure 2). The intricate structure of this model produces very realistic seismic data, causing problems for some migration methods. Even when the correct velocity model is used, many migration methods cannot completely image the target structure, while other methods have little trouble producing a nearly perfect image. The large number of thin layers in the Marmousi velocity model also causes problems when doing velocity estimation. It is difficult to estimate a blocky velocity model for migration that looks geologically reasonable but still honors the actual velocities well enough to produce a good image. This extremely successful data set continues to be used as a testbed for migration and velocity estimation methods (Versteeg, 1994). As expensive as this data set was to design and produce, the total cost averaged over all the times it has been used to test algorithms yields an average cost that can be no more than pennies, certainly one of the most worthwhile investments in the history of seismic R&D.

While the Marmousi model has been an excellent test data set for the industry, it is not sufficient for testing all migration techniques. Its primary limitations are that the model is two dimensional, acoustic, and isotropic. Modern seismic-migration techniques are developed to address data in three dimensions, with the additional potential complexities of anisotropy and elasticity. Although no synthetic three-dimensional model with Marmousi's level of stratigraphic detail has been produced, there are a few three-dimensional prestack structural model data sets, e.g., the SEG-EAGE salt model shown in Figure 3 (Aminzadeh et al., 1994). We need three-dimensional models because extending our migration techniques, especially prestack, from two to three dimensions is nontrivial—not just

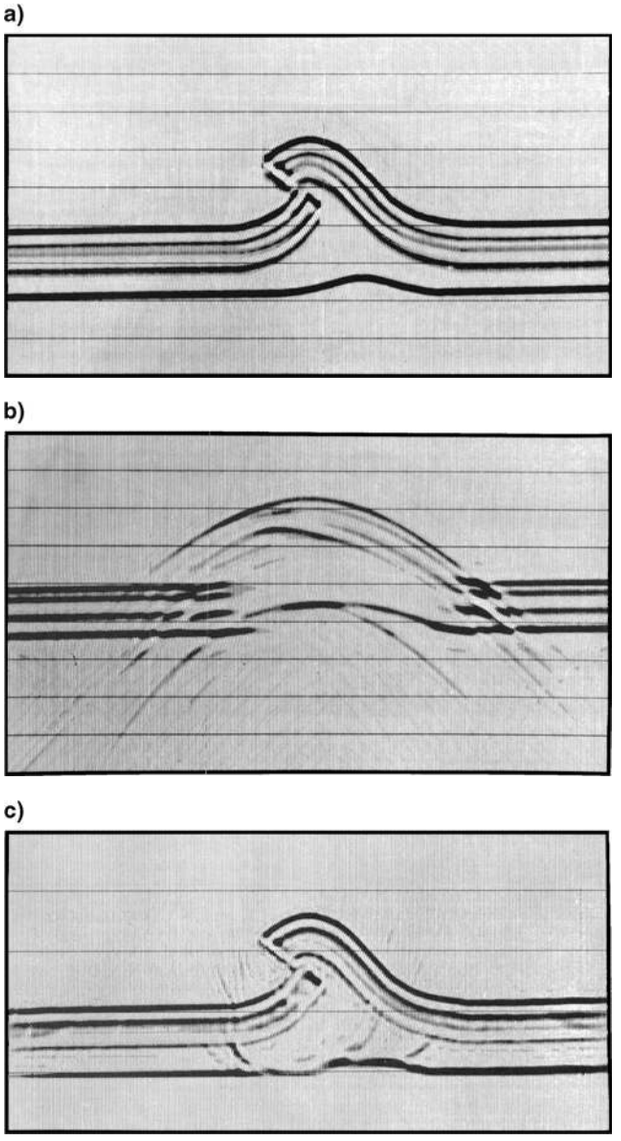

FIG. 1. (a) The overthrust model, expressed as seismic traces. The values on the traces are the derivatives of the velocities. (b) Exploding-reflector synthetic seismic data from the overthrust model. (c) Reverse-time migration of the data. The migration has imaged the structure nearly perfectly; the minor artifacts appearing on the image are due to inaccuracies in the modeling program. (From Baysal et al., 1983.)

a simple matter of adding an extra program loop to handle the action of migration away from a single plane of acquisition.

We also need anisotropic models in order to test the ability of our migration and velocity-estimation techniques to handle anisotropy. To date, very few anisotropic model data sets have been publicly released. One anisotropic model, which is meant to investigate the behavior of seismic waves around a thrusted shale layer (as encountered frequently in the Canadian Foothills), has appeared both as a physical model data set (Leslie and Lawton, 1998) and a F-D synthetic data set (Fei et al., 1998). Figure 4 shows images of the synthetic data set migrated using isotropic and anisotropic migration algorithms. Although the anisotropy (tilted-axis transverse isotropy) in this model is rather weak, neglecting it, as in the isotropically migrated image in Figure 4a, can lead to an incorrect structural interpretation beneath the thrust sheet.

TIME MIGRATION, DEPTH MIGRATION

A frequent query regarding migrations asks, "Is this a time migration or a depth migration?" We take the view that, roughly speaking, "time migration" refers to migration algorithms that pay no attention to ray bending, and "depth migration" refers to algorithms that do honor ray bending. The distinction between time and depth migration is actually more vague than that, for some consider $v(z)$ migrations such as phase-shift migration (Gazdag, 1978), which honors ray bending, to be time migration, while others consider time migration followed by image-ray conversion (Larner et al., 1981) to be a depth migration process. In practice there is a sizeable "gray area" between time and depth migration. In some ways, the distinction between them is artificial, but in other ways, it is very real. Both have their uses. The true earth coordinates are of course in depth, not time. Even so, interpreters often need data in time coordinates, because the standard interpretation systems, log synthetics, and seismic-attribute techniques work with time and frequency, not depth and wavelength.

The most apparent (and superficial) difference between time and depth migration occurs in the final display of migrated traces. Time migration produces a time section that interpreters can compare relatively easily with unmigrated time sections. On the other hand, time migration can be converted to depth using velocity information, and depth migration can be displayed using a vertical traveltime coordinate system. Fundamentally, though, geologists and engineers think in depth and prefer to see a seismic section displayed in depth in order to compare with geologic structure. Often, stretching the migrated traces is enough to convert from time to depth, but in regions with lateral velocity variation, a simple stretch is not enough. In fact, it is often necessary to perform both time migration and depth migration on the same survey, for they both provide useful (though sometimes apparently conflicting) information.

The greatest real difference between the actions of time and depth migration lies in how they use velocity. Time migration, following the tradition of NMO and stack, uses an imaging velocity field, i.e., one that best focuses the migrated image at each output location. This velocity field is free to change from point to point, so that time migration, in essence, performs a constant-velocity migration at each image point, where the constant changes from point to point. This potentially inconsistent treatment of the velocity field makes time migration

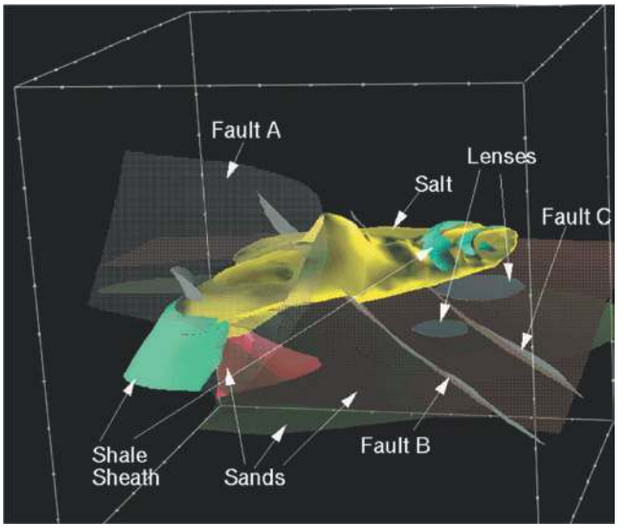

FIG. 3. The salt body and several reflecting horizons from the SEG/EAEG three-dimensional salt model. (Courtesy SEG/EAGE 3D-modeling committee.)

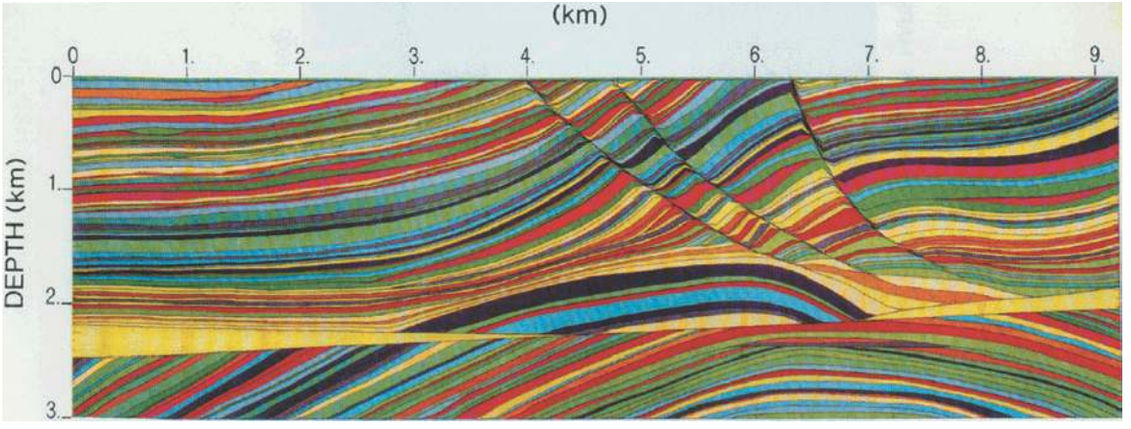

FIG. 2. The Marmousi velocity model. (From Versteeg and Grau, 1991.)

appear puzzling, or even nonsensical, from the point of view of migrating surface-recorded reflection data to points inside the earth using the wave equation. By pursuing the analogy with NMO/stack, however, we can view time migration as a valid imaging process, as long as we don't place too much faith either in its ability to migrate events to their correct locations or in the "velocities" that we derive. In fact, we can view time migration, performed before stack, as the generalization of NMO/stack that includes all dips, not just flat ones, while also collapsing diffraction energy. This is true in the sense that a prestack time-migration program restricted to imaging only flat dips at source-receiver midpoint locations will yield an image that is identical to a stacked, unmigrated section. As with NMO/stack, the imaging velocity field used for time migration is not required to relate to the true geological velocity field in any way. In fact, assuming that the imaging velocities are actually root-mean-square (rms) velocities and using Dix's equation (Dix, 1955) to invert these to interval velocities often produces physically impossible values for velocity. This inconsistency should not concern us; *the goal of time migration is to produce an image, not a geologically valid velocity field!*

Depth migration, in contrast, uses an interval velocity field, i.e., a model of the earth's subsurface. The interval velocities used are averages of the actual earth velocities, where the average is taken over some characteristic distance such as a wavelength. This allows depth migration to model seismic wave behavior within the earth much more accurately than time migration can. In particular, it allows us to use depth migration, especially depth migration before stack, as a velocity estimation tool.

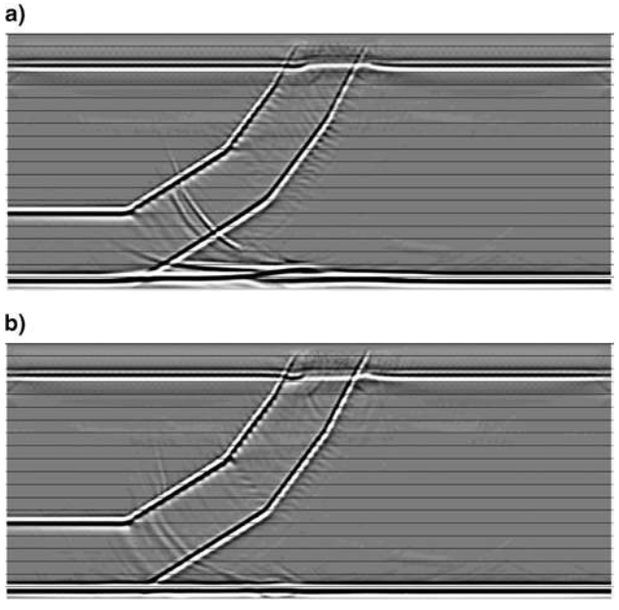

FIG. 4. (a) Isotropic prestack-migrated image of data from an anisotropic F-D model of a thrust sheet. The incorrect handling of the weak velocity anisotropy within the thrust sheet has caused the appearance of a false structure beneath the sheet. (b) Anisotropic prestack-migrated image of the same data. The false structure has been removed by accounting for anisotropy within the (Kirchhoff) migration algorithm. (Images courtesy of Veritas DGC Inc. Synthetic data used as input to the migration courtesy of BP.)

The usual technique is to perturb the velocity field until a model is obtained that looks "geologically plausible" and produces a good stacked migrated image, with events in the prestack-migrated common-image-point gathers as flat as we care to make them. The velocity updates may be made using simple velocity semblance scans, more sophisticated tomographic velocity analysis techniques, manually (driven by a geological model), or (most often) some combination of all of these. Unfortunately, an incorrect velocity model may still produce a good image with flat gathers (Stork, 1992). And, for migration (as opposed to migration/inversion), if the velocity field lenses rays, causing multipathing, even the correct velocity model may not produce uniformly flat gathers (Nolan and Symes, 1996). In practice, geological information should be used to guide the velocity-estimation process, helping to ensure that the final result will be "geologically plausible." Depth migration can be as much of an interpretative process as it is a computational exercise.

Using depth migration to estimate velocity has turned out to be one of the hardest problems facing geophysicists, which is one reason why so many geophysicists prefer time migration. Several years ago, prestack depth migration was expected to improve the accuracy and reliability of velocity estimation to the point that typical velocity errors would be 5% or less. This has not yet generally happened, which is disappointing because industry is still plagued by persistent misties, both horizontally and vertically, for wells drilled into structural targets. Improper treatment of velocity anisotropy has certainly been part of the problem (Banik, 1984), and improved estimation of anisotropic velocities may yet improve the situation. Given the correct velocities, depth migration ought to be able to produce an accurately positioned structural image. Its frequent inability to predict accurate target locations in practice does not represent an inherent failure of the method, but rather a shortcoming in our ability to perform velocity estimation. Even given an imperfect velocity field, depth migration's underlying physical basis enables it to produce images that are more structurally correct than time migration is capable of (see Figure 5 for an example). Depth migration's use of physically meaningful velocities also provides a quality check for depth migration that is unavailable with time migration.

Depth migration is more ambitious than time migration, and it hasn't always lived up to expectations. With its twin objectives of imaging and velocity estimation, depth migration is inherently more difficult than time migration, which can usually produce acceptable imaging results fairly quickly. However, depth migration is a more powerful interpretive processing tool, and its results can give us greater confidence in both the geologic structure and the velocity field than the results of time migration can.

MIGRATION METHODS

In this section, we describe some of the major migration methods. The theory of all these methods has been presented elsewhere (Gardner, 1985; Yilmaz, 1987; Whitmore et al., 1988), especially for poststack migration. Instead of rehashing the theory, we concentrate on describing the range of practical problems faced by these methods, especially in their prestack implementations. We also emphasize the development of the methods in depth rather than time.

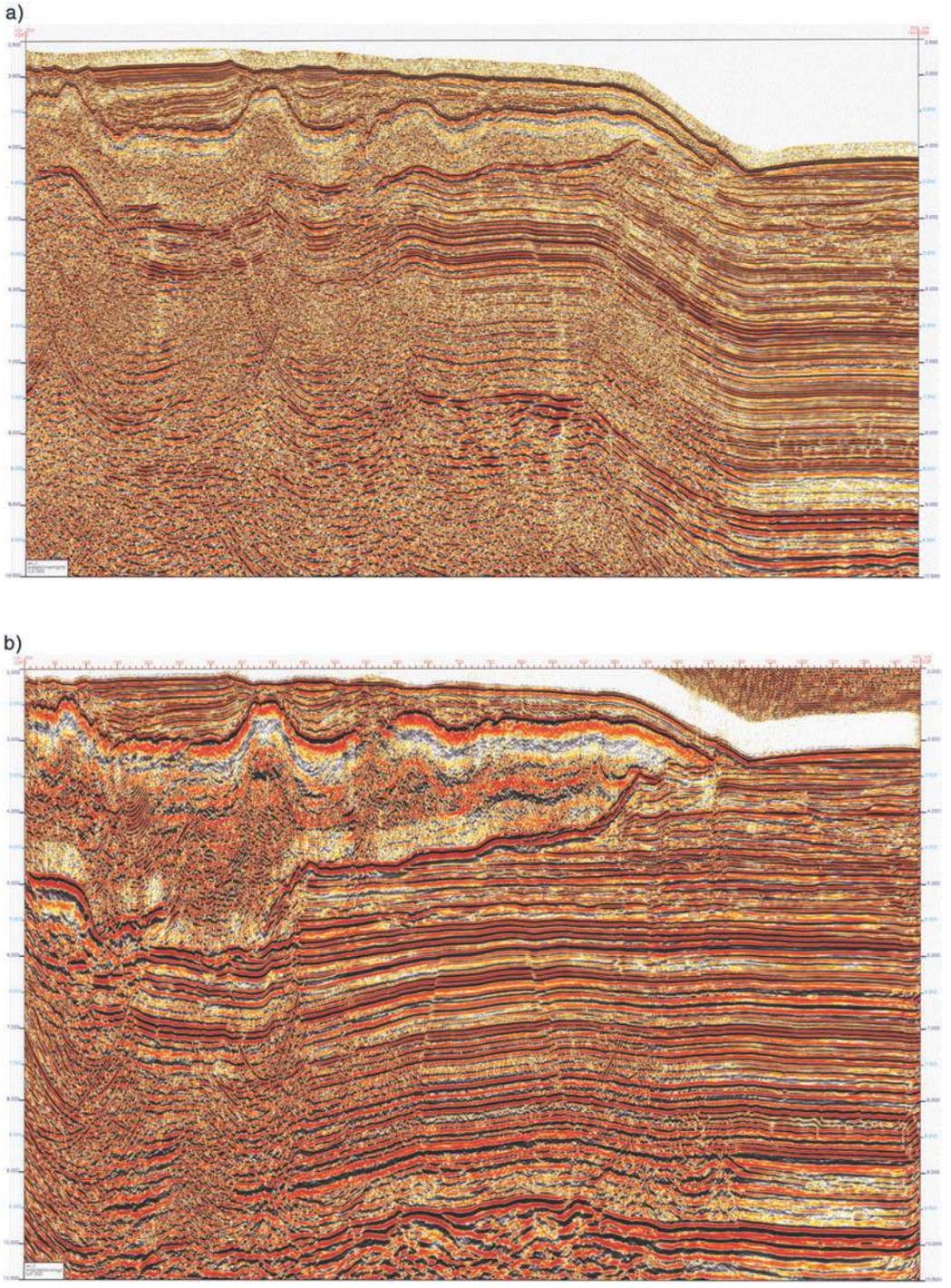

FIG. 5. (a) Prestack time-migrated image of a Gulf of Mexico salt body, showing the effects of the high-velocity salt on the image quality and structure location of the underlying lower velocity sediments. (b) Prestack depth-migrated image from the same location showing improvements in image quality and structure location. (From Young et al., 1999. Images courtesy of Veritas DGC Inc.)

Kirchhoff migration

The easiest method to describe kinematically is Kirchhoff migration. Given a source location and a receiver location (both on the earth's surface), a sample at time t on a primaries-only unmigrated trace might contain energy reflected from any point in the earth for which the total traveltime from source to reflector to receiver is t. In a constant-velocity earth, this locus of points is the bottom half of an ellipsoid in three dimensions (or an ellipse in two dimensions) with a focus at the source and

a focus at the receiver. In the further special case of a coincident source-receiver pair, the ellipsoid becomes a sphere (and the ellipse becomes a circle). These are the only candidate reflector locations. With only this information (a single spike on an unmigrated trace), migration has no choice but to spread out the spike over the locus of all possible reflection points—the bottom half of the ellipsoid. Figure 6 shows an example. Given a different sample, perhaps on a different unmigrated trace, migration would similarly spread that sample onto an ellipsoid of its own. Kirchhoff migration works by repeating this process for all samples on all input unmigrated traces, summing each resulting ellipsoid's contributions into the output image as it goes.

Of course, there is much more to Kirchhoff migration than this. Schneider (1978) provided a firm wave-equation basis for Kirchhoff migration, and Bleistein (1987) extended that theory to include the ability to solve for reflectivity, thus paving the way for parameter estimation after migration. But kinematically, the above is an accurate description of constant-velocity migration [embodied mathematically in equation (1) below], and many migration algorithms do work this way.

It is also possible to consider each image point as a possible diffractor of seismic energy. This is the wave-equation-based successor to the classical diffraction stack method (Miller et al., 1987). In this formulation (the one more commonly used in practice), the algorithm constructs its output one image point at a time, calculating for each input unmigrated trace at what time a diffraction from a hypothetical scatterer located at that image point would have arrived. The data sample with that arrival time is then summed into the output image point. Accumulating the sum over all the traces within the migration aperture completes the calculation for that image point. In the 2-D zero-offset constant-velocity case, each output image point requires a summation over a hyperbolic trajectory through the data—the familiar curve of a point diffractor. Figure 7 shows an example.

Computationally, the heart of the constant-velocity Kirchhoff migration program requires each input (unmigrated) trace to visit each output (migrated) sample within a migration aperture exactly once. This fact allows us to estimate fairly accurately the number of additions that will be performed in the migration program—simply the number of output samples multiplied by the number of input traces. If we find that this number of additions is larger than acceptable, we have the option to reduce either the number of output samples or the number of input traces.

Kirchhoff migration is conceptually simple, and it is very versatile. These properties alone do not guarantee that Kirchhoff migration will be accurate. However, it has proven to be remarkably accurate in a wide variety of imaging applications, despite its obvious theoretical shortcomings, two of which we describe next.

First, almost all implementations of Kirchhoff migration make use of an asymptotic approximation that is valid only for large values of ω times t, where ω is angular frequency and t is traveltime. This range of validity means that diffractors within several wavelengths of source or receiver locations will not be imaged correctly. At the very least, this high-frequency approximation casts doubt on our ability to image accurately in the near surface. In practice, only the shallowest depths, within a few wavelengths of the source and receiver locations, are affected by this approximation. Usually, even these locations are reasonably well imaged, albeit with some degradation of the amplitude and phase.

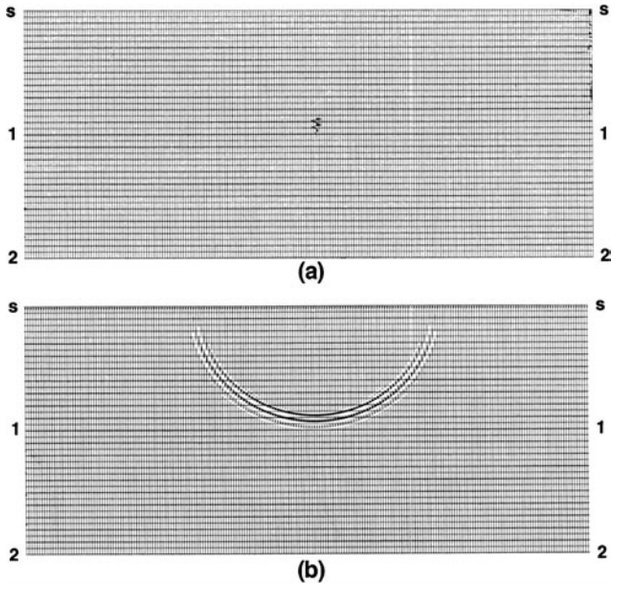

FIG. 6. Migration principle based on smearing. (a) An unmigrated zero-offset section, consisting of a single nonzero sample on the central trace. (b) Migrated section, showing that the spike gets smeared onto the locus of possible reflection points (for this constant-velocity zero-offset 2-D example, a semicircle). (From Yilmaz, 1987.)

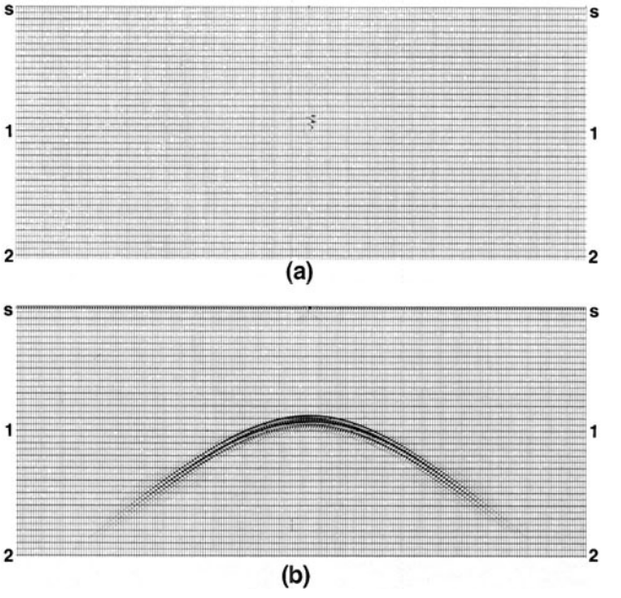

FIG. 7. Migration principle based on diffraction summation. (a) An idealized cross section, consisting of a single point scatterer in an otherwise homogeneous earth. (b) The zero-offset response to the cross section, consisting of a single diffraction curve (for this constant-velocity zero-offset 2-D example, a hyperbola). Kirchhoff migration performs a weighted sum of the amplitudes along the diffraction curve and places the sum at the scatterer location. (From Yilmaz, 1987.)

The second weakness of Kirchhoff migration, which arises when the velocity is not constant, is related to the first. Because of the high-frequency approximation, propagation distances between diffractors and sources or receivers are limited to be large, i.e., more than a few wavelengths. We are not permitted to take the wavefield observed at the receivers and continue it a short distance into the earth; we may only continue it a large distance. However, there are many possible travelpaths for seismic energy to take as it travels a large distance from one location to another, and no implementation of Kirchhoff migration has yet accounted with complete success for the problem of an unlimited number of travelpaths. Instead, all Kirchhoff migration programs assume that energy propagates along at most a few travelpaths (usually one) between any two points. Figure 8 illustrates this multipathing problem in two dimensions.

The restriction to one or a few travelpaths also provides Kirchhoff migration with one of its greatest strengths. It allows Kirchhoff migration with a laterally varying velocity field to run considerably faster than other methods, at least in most cases, while preserving its flexibility. The most popular competing methods that can handle lateral velocity variations accurately are the wavefield continuation methods. By their very nature, these methods take the wavefields from the source and the receivers and extrapolate them, one depth step at a time, into the earth. These methods are recursive, because they recompute the wavefield at each depth, based on the wavefield at the previous depth. By contrast, Kirchhoff migration is nonrecursive, because it computes the wavefield (or image) at all depths directly from the wavefield at the recording surface. Figure 8 illustrates this point. Although wavefield-continuation methods account for all possible propagation paths within their cone of propagation validity, which tends to be dip limited, their operation also tends to be more time-consuming than Kirchhoff migration.

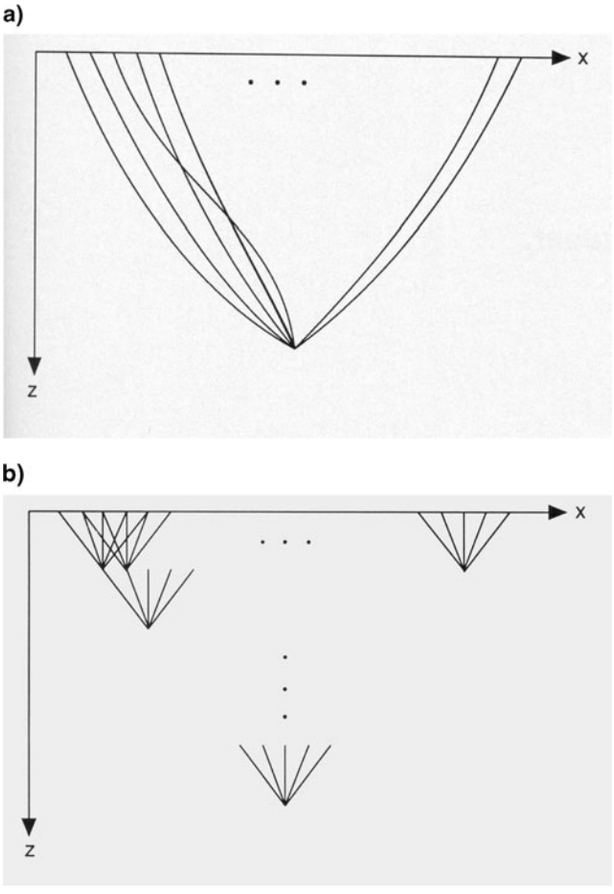

FIG. 8. (a) Propagation paths (raypaths) from the recording surface to an image location. Although there may be several raypaths between a surface location and an image location, most Kirchhoff migration programs use only a few (usually one). (b) Propagation paths from the recording surface through intermediate points to an image point. Here, many paths join a surface location and the image point. Wavefield continuation methods account for all these propagation paths, making them generally more accurate than Kirchhoff migration. (From Gray and May, 1994.)

The major advantages of Kirchhoff migration over other methods are its flexibility and its ability to handle lateral velocity variations with relative efficiency. Its ability to handle lateral velocity variations accurately is another matter. We have seen that Kirchhoff migration can be no more accurate, at least for moderate dips, than the wavefield-continuation methods. Surprisingly, there is also a fairly wide range of accuracy for different implementations of Kirchhoff migration. This is a result of the many types of traveltime solvers currently used, ranging from simple solutions of the eikonal equation (e.g., Vidale, 1988) to amplitude- and phase-preserving dynamic raytracing. Audebert et al., (1997) give a good summary of those approaches and, applying them to the Marmousi model, present several imaging comparisons.

In addition to its theoretical shortcomings, Kirchhoff migration has two major practical disadvantages relative to other methods. The first, described above, is its relative lack of accuracy, and the second is its susceptibility to operator aliasing. The problem of operator aliasing arises naturally for Kirchhoff migration, which images by passing a diffraction surface over data without regard for their frequency content. As Abma et al. (1999) explain, the steep part of a diffraction surface can easily undersample the seismic wavelet as it passes over a flat portion of the unmigrated data. To overcome this problem, Gray (1992) and Lumley et al. (1994) proposed reducing the frequency content of the data encountered by the steep part of the diffraction surface. This approach works well (Figure 9), but it adds a certain amount of complexity and expense to the migration.

The first problem, that of accuracy, has been attacked with some success by several approaches that maintain the flexibility of Kirchhoff migration. We mention two of these approaches. Gaussian beam migration (Hill, 1990, 2001) performs local decompositions of the source and receiver wavefields into "beams," and directs those beams back into the earth using extremely accurate ray tracing. Several beams can emanate from a given surface location, with the different beams referring to different initial propagation directions. Each beam propagates independently of all the others, guided by an individual ray tube (Figure 10). The ray tubes can overlap, so that energy can travel between image locations and source and receiver locations by more than one path. This allows Gaussian beam migration to address the multipathing problem. Figure 11 shows a Marmousi image produced by this method. This image is clearly superior to every published single-arrival Kirchhoff-migrated image from the same data set.

Bevc (1997) proposes a different solution of the multipathing problem. This method begins by applying standard Kirchhoff migration (nonrecursively) down to a depth many wavelengths below the recording surface. Within that restricted depth range, the method assumes that multipathing has not yet become a severe problem, so that Kirchhoff migration has performed accurately. At that depth, the method computes a downward-continued wavefield, also by Kirchhoff methods (Berryhill, 1984), and that wavefield is used for Kirchhoff migration within the next restricted range of depths. After several of these combined operations of migration and downward continuation, the process is complete. This method allows for multipathing by cascading together several steps of single-path propagation. However, it has proven practical to date only in two dimensions.

In building a new migration program to be used perhaps thousands of times on large volumes of data, one must decide which algorithm to use. Before writing a Kirchhoff migration program, one must weigh its advantages against its disadvantages, and decide whether the savings gained from its repeated use exceeds the value of the time spent writing a detailed, complicated computer program containing accurate amplitude and traveltime calculations and effective anti-aliasing. As computation speed increases, improving the economics of other migration methods relative to Kirchhoff migration, these decisions are becoming much harder than they were a few years ago.

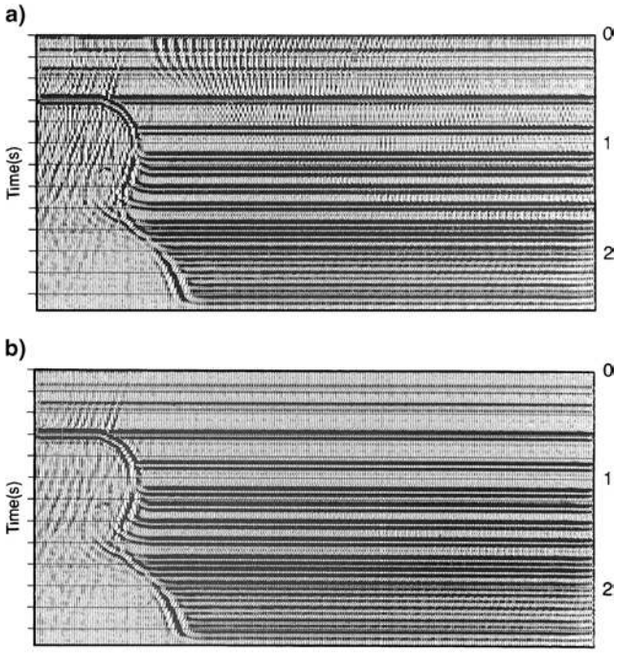

FIG. 9. (a) Kirchhoff-migrated image of a steeply dipping salt flank. No attempt has been made to suppress the artifacts due to operator aliasing. (b) The same image, with operator aliasing effects suppressed. (From Gray, 1992.)

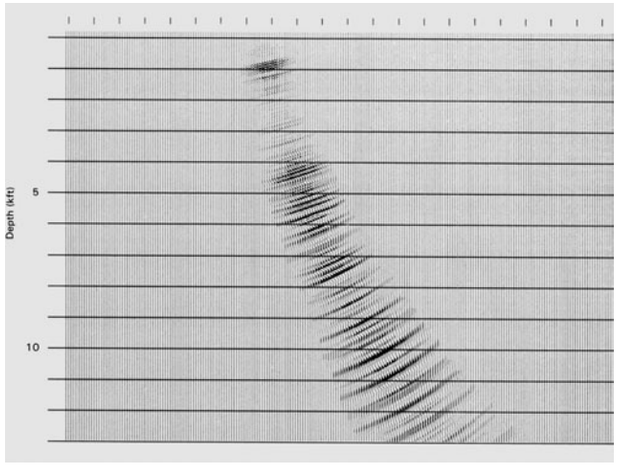

FIG. 10. The contribution of the region around a single raypath to a poststack-migrated image in Gaussian beam migration. (From Hill, 1990.)

Finite-difference migration

Most Kirchhoff migrations form the image at output locations by summing data over input locations. Mathematically, this can be expressed as a spatial convolution. For example, constant-velocity 3-D poststack Kirchhoff migration gives the migrated image P at a point (x, y, z) as

$$P(x, y, z, t=0) = \int W(x-x', y-y', z) \times P'(x', y', z=0, t=r/v)\, dx'dy'. \quad (1)$$

In equation (1), W is a weight function, v is the half velocity, r is the distance between the surface location $(x', y', 0)$ and the image location (x, y, z), and the prime on the surface- recorded wavefield P indicates time differentiation. Using equation (1), we can compute the image at whatever image locations we choose. As previously noted, however, equation (1) is not an exact expression for the migrated wavefield; it lacks a term that rapidly decays relative to the derivative P' as the migration depth increases away from the recording surface. Figure 8(a) indicates the convolution of equation (1) schematically in two dimensions; each point in the image is directly calculated in a single global summation over the data recorded at the surface.

Figure 8(b) analogously indicates the operation of a wavefield-continuation method, explicit finite-difference migration

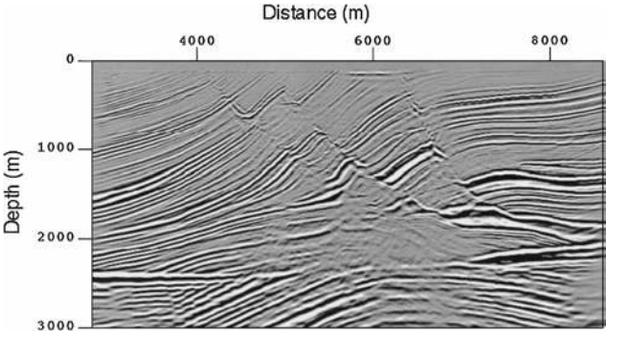

FIG. 11. Gaussian beam migrated image of the Marmousi data set. (From Hill, 2001.)

(Berkhout, 1984). As can be seen from the figure, this method is based on repeated application of a local convolution:

$$p(x, y, z + \Delta z, \omega) = \int w(x - x', y - y', \Delta z)\, p(x', y', z, \omega)\, dx'dy', \quad (2)$$

where $p(\omega)$ is the temporal Fourier transform of the wavefield $P(t)$. Equation (2) is an expression for downward continuing a single frequency component of a wavefield, one either generated by a source or recorded by receivers. The velocity is contained in the weight function w, which is the Green's function for wavefield extrapolation in depth. The method is recursive, using equation (2) to compute the wavefield at each depth $z + \Delta z$ from the wavefield at the previous depth z. As can be seen from Figure 8(b), this incremental approach naturally allows for multiple travelpaths between a possible diffractor at depth and each source or receiver.

Explicit F-D prestack migration is a two-step process. First, the wavefields from the source (modeled from the known source geometry) and from the receivers (the recorded seismic data) are downward continued to all depths in the earth via equation (2). (Note the extrapolation operators are slightly different for the source and receiver wavefields. For the source, the extrapolation proceeds in the direction the waves traveled; for the receivers, it is opposite to the direction the waves traveled.) At each depth, the downward-continued wavefields are then combined to produce an image, using the principle that the source wavefield excites a corresponding time-coincident receiver wavefield at a reflector (Docherty, 1991). By carefully accounting for such factors as geometrical spreading and source and receiver illumination in the imaging condition, it may also be possible to improve the calculated amplitudes. How best to accomplish "true-amplitude migration," however, will depend both on the survey geometry and practical considerations.

A few words about the practical implementation of explicit F-D migration are in order. The convolution in equation (2) takes place, in principle, over an infinite spatial range. Truncating this aperture, as we must do in practice, easily leads to numerical instability. A careless implementation can yield images that are accurate down to depths of some tens of wavelengths, but with errors that grow exponentially below that. There are ways around this problem, of course, or the method would not be viable (Holberg, 1988; Hale, 1991a), but the stability comes at the price of limiting the method's ability to image the steepest dips.

In practice, we always approximate w in equation (2) with a constant-velocity Green's function, using the velocity at the center of each extrapolating fan, $v(x, y, z)$, as the "constant velocity" for that extrapolation. Fortunately, explicit F-D migration usually works quite well in practice despite the mathematically inconsistent treatment of velocities this approximation implies; the wavefield effectively "heals over" the local irregularities thus introduced. For strong lateral velocity contrasts, however, even the "guaranteed stable" versions of the method can become unstable and fail, so some care should be taken when generating the velocity field before migration (Etgen, 1994).

The term "explicit" suggests there should also be "implicit" F-D wavefield-continuation migration methods. In fact, the first digital wave-equation-based migration method was implicit F-D migration (Claerbout and Doherty, 1972). There are both time-domain and frequency-domain versions of this method. Mathematically, "explicit" and "implicit" merely refer to different techniques for numerically solving differential equations, but in the migration literature the terms also refer to the type of wave equation being solved. Instead of starting from the actual acoustic or elastic wave equation and then approximately solving it (the approximations being necessary to avoid instability), implicit methods solve an approximate "one-way" wave equation that supports only inherently stable solutions by design (Yilmaz, 1987). One-way wave equations are all-pass filters, with no evanescent regions. For waves propagating downward or close to downward, one-way wave equations and the exact wave equation behave similarly, but their behaviors progressively deviate for propagation at steeper dips.

Both the implicit and the explicit finite-difference methods are accurate for a restricted range of dips, and their accuracy can be improved at steep dips (though not to vertical dips) with a certain amount of extra work. They are both wavefield-continuation methods, lacking the flexibility of Kirchhoff migration, but supporting multipathing. Are they cheaper or more expensive than Kirchhoff migration? It is impossible to answer that question definitively in all cases, because the answer depends on the application (2-D versus 3-D, prestack versus poststack).

The expense of any migration method depends on many factors, including frequency content of the seismic data and the maximum dip to be imaged. For example, clearly the expense of frequency-domain methods is proportional to the number of frequencies involved, because each frequency component of the wavefield is imaged separately. Less obvious is the fact that the expense of Kirchhoff migration also depends on the frequency content. Roughly speaking, the cost of Kirchhoff migration is linearly proportional to the maximum frequency, because the maximum frequency helps to determine the depth resolution of the image, and hence the maximum depth-step size allowed. This fact is also true of frequency-domain migrations, however, so the expense of frequency-domain migrations depends in two ways on the frequency content, making its dependence on maximum frequency quadratic, not linear. That is just one example of the subtle difficulties in determining the relative expense of migration methods.

A more striking difference between standard Kirchhoff migration and wavefield-continuation methods [specifically F-D migration, but also including integral methods such as Bevc's (1997) algorithm] can be seen in their treatment of migration aperture. Summing input traces over a diffraction curve or smearing input samples onto an output aperture is the major action of Kirchhoff migration. If a larger aperture is needed, an individual trace swings into more output traces. F-D migration, on the other hand, continues entire wavefields downward from the recording surface. If a larger aperture is needed, this aperture must be included as part of the entire calculation. In other words, the migration must include the aperture (output traces) at all depths, even if no energy is present at the recording surface at those trace locations. For example, in common-shot migration, the source wavefield is excited at a single lateral location, but the downward continuation of that wavefield spreads the energy into many lateral locations. Traces at these locations must be included in the downward continuation, even though no energy is present at those locations at shallow depths

(Figure 12). This simple fact typically results in an enormous number of extra calculations for F-D migration, and has so far made 3-D prestack migration of marine streamer data by F-D methods economically uncompetitive compared to Kirchhoff methods.

For 3-D poststack migration, the situation is quite different. The problem of padding extra traces to fill out the migration aperture doesn't exist, and F-D migration, at least out to moderate dips, is typically cheaper than Kirchhoff migration. One explicit F-D method, Hale-McClellan migration (Hale, 1991b), can even be cheaper than Kirchhoff methods for imaging moderate to steep dips. Li (1991) has improved the accuracy and performance of 3-D implicit F-D migration, and this improvement can be adapted for explicit migration as well (Etgen and Nichols, 1999). (Once again, we emphasize the subtle issues in estimating migration cost. We cannot say categorically that every 3-D Hale-McClellan poststack migration will be cheaper than the corresponding 3-D Kirchhoff migration; we can only give the cost comparison for a wide range of typical migration jobs.)

Reverse-time migration

Another method uses finite differences to solve the wave equation, but instead of extrapolating in depth (requiring choosing whether the waves being extrapolated are upgoing or downgoing), it solves the full (two-way) acoustic or elastic wave equation by extrapolation in time, allowing waves to propagate in all directions. This method is called reverse-time migration. We described reverse-time migration briefly in the section on seismic modeling: reverse-time migration is just F-D wave-equation modeling run in reverse (Figure 13). Baysal et al. (1983) and McMechan (1983) present the method in detail and describe its ability to image all dips with great accuracy.

Reverse-time migration has the same problems with stability and numerical dispersion that finite-difference modeling has; it is straightforward (but expensive) to control these problems. The cost of reverse-time migration is also easy to determine. For each shot gather, it is proportional to the product $N_t \times N_x \times N_y \times N_z \times N_{fd}$, where N_t is the number of time steps taken, $N_x \times N_y \times N_z$ is the number of grid points on which the wave equation is being solved, and N_{fd} is the number of points used in the local F-D operator. To properly sample the wavefield, the size of the grid cells must decrease as the maximum frequency of the data increases. For stability reasons, the size of the time steps must decrease as the size of the grid cells decreases. For 3-D problems, the cost is thus proportional to the fourth power of the maximum frequency. Just as 3-D F-D

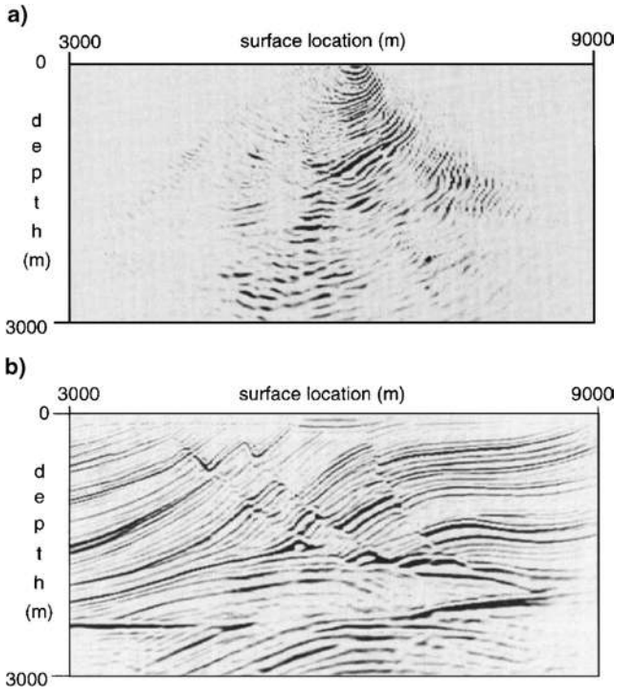

FIG. 12. (a) A single finite-difference-migrated shot record from the Marmousi data set. Although the input record is localized in space, the migration aperture is much larger, increasing the cost of the migration. (b) Stack of all the finite-difference-migrated shot records from Marmousi. (From Ehinger et al., 1996.)

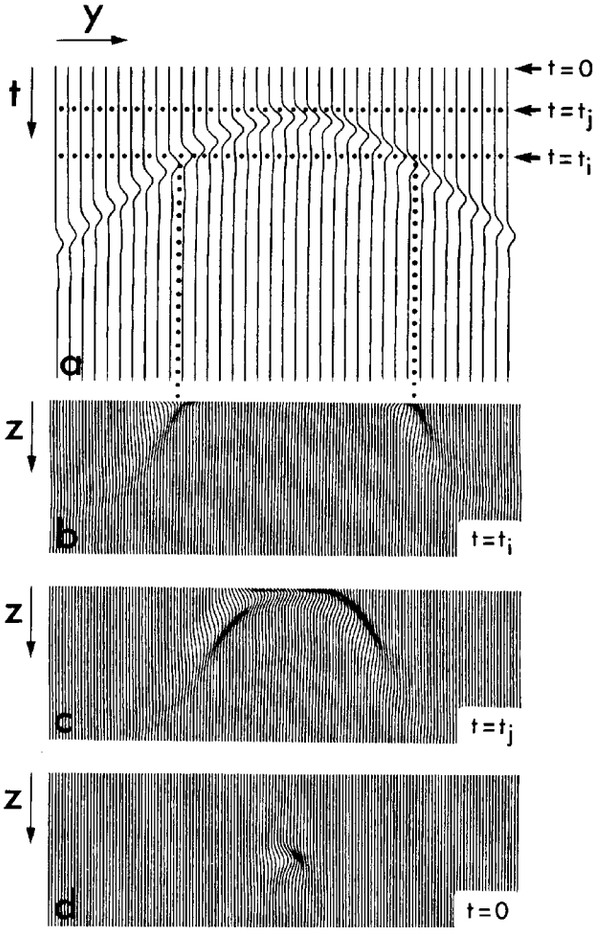

FIG. 13. The principle of reverse-time migration. The wavefield recorded at the surface is fed back into the earth using the wave equation with time running backwards. Snapshots at earlier times show the wavefield closer to its initiation in time and space and, for poststack migration, the snapshot with time equal to zero shows an image of the exploding reflectors. (From McMechan, 1983.)

shot-record modeling is extremely expensive, 3-D reverse-time shot-record migration is also. Prestack reverse-time migration also has the same drawback of having to pad the recorded traces out to the full migration aperture, greatly increasing the expense if the required aperture is large.

Still, reverse-time migration is potentially the most accurate method in the sense of faithfully honoring the wave equation, and all other methods eventually fall short of it in their approximations. It is legitimate to ask whether the accuracy of reverse-time migration is ever needed, especially given typical uncertainties in migration velocities. Reverse-time migration's greater accuracy does demand correspondingly greater care in its use. These concerns are all the more valid given (1) the very high accuracy of the other F-D migration methods, and (2) the potential of generating unwanted artifacts, for example, internal multiples from locations of sharp impedance contrasts.

Frequency-wavenumber migration and its extensions for laterally varying velocity

So far, we have discussed methods that operate in space and time (Kirchhoff and reverse-time), and in space and frequency (explicit F-D and some implementations of implicit F-D). Next, we describe methods that operate in wavenumber and frequency, and some of their extensions that can handle lateral velocity variations.

Stolt (1978) and Gazdag (1978) introduced two poststack migration methods that are strictly valid for vertical velocity variations at most. They make up for their lack of flexibility by being extremely fast, and they have become workhorses. Both methods begin by Fourier transforming the input traces from their original space and time coordinates (t, x, y) into monochromatic plane-wave components (ω, k_x, k_y). This is a useful transformation, because in the Fourier domain the constant-velocity wave equation becomes a simple algebraic identity relating the temporal frequency ω and the wavenumber components k_x, k_y, and k_z of the monochromatic plane waves. Stolt migration uses this relationship to move the amplitude and phase at each (ω, k_x, k_y) to their corresponding (k_z, k_x, k_y) location, downward continuing and imaging in a single step. After interpolation onto a regular grid, inverse Fourier transformation to (z, x, y) then produces the desired space-domain image.

Gazdag's phase-shift migration is slightly more complicated, performing a separate downward continuation of each (ω, k_x, k_y) component from one depth to the next. The downward continuations have the form of phase rotations, and are given by

$$\tilde{p}(k_x, k_y, z+\Delta z, \omega) = \tilde{p}(k_x, k_y, z, \omega) \exp\left\{ i\Delta z \sqrt{\frac{\omega^2}{v^2} - \left(k_x^2 + k_y^2\right)} \right\}, \quad (3)$$

where $\tilde{p}$ is the spatial and temporal Fourier transform of the wavefield P, and v is the velocity between depths z and Δz. Because of its recursive design, phase-shift migration naturally honors Snell's law, with the plane wavefronts changing dip as they propagate through the $v(z)$ earth. This makes phase-shift migration an extremely powerful tool for accurately imaging steep-dip intrusions in sedimentary basins such as the Gulf of Mexico. In fact, phase-shift migration has been extended to image greater than vertical dips in areas with a laterally invariant background velocity (Claerbout, 1985, 272–273). Figure 14, from Hale et al. (1992), shows clearly imaged overhung salt faces from a 3-D survey using this method.

Clearly, (ω, k_x, k_y) methods that can efficiently produce images such as Figure 14 are extremely powerful. They have become the basis for many poststack and prestack time-migration methods in common use where it is more important to see an image than to be able to pinpoint the exact location of all its features. These methods are limited in their applicability as depth migrations, though, because of their inability to handle laterally varying velocities. Two extensions of phase-shift migration have seen a great deal of use as poststack depth migrations, however. Both use Fourier transforms to go back and forth between the wavenumber and space domains, and a large part of their expense is taken up by these transforms.

First, Gazdag and Sguazzero (1984) developed a method called phase-shift-plus-interpolation (PSPI) migration. This method downward continues and images a Fourier-transformed wavefield just as phase-shift migration does, except that PSPI does each downward continuation from depth z to depth $z+\Delta z$ multiple times for a range of different velocities v. Each of these wavefields is then inverse Fourier transformed from frequency-wavenumber (ω, k_x, k_y) to frequency-space (ω, x, y). A single wavefield at the depth $z+\Delta z$ is then constructed by interpolating between the available constant-velocity extrapolations, using the velocity at each (x, y) location to guide the interpolation. This single combined wavefield is then transformed back to wavenumber, and the downward continuation continues. The more velocities used in the phase-shift downward continuations, the greater the accuracy of PSPI will be, and the more expensive it will be [because of the cost of the inverse Fourier transforms from (ω, k_x, k_y) to (ω, x, y)]. Typically, this is a very expensive, very accurate depth migration method. Patching together constant-velocity solutions is still an approximation, however, and if the lateral velocity variation is strong enough, PSPI can become noticeably unstable as a result (Etgen, 1994).

Next, split-step migration (Gazdag and Sguazzero, 1984; Stoffa et al., 1990) is a more efficient, but somewhat less accurate, alternative to PSPI for 3-D depth migration. Like phase-shift migration, split-step migration extrapolates the Fourier-transformed wavefield from one depth level to the next using

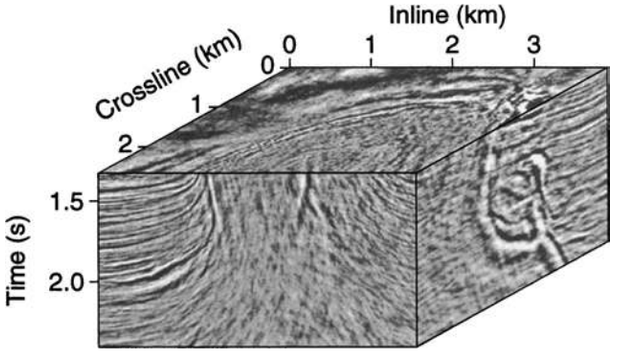

FIG. 14. Three-dimensional phase-shift-migrated image of a salt dome, showing overturned salt faces. (From Hale et al., 1992.)

one laterally invariant velocity. Unlike phase-shift migration, it then perturbs this result to account for lateral velocity variations by inverse Fourier transforming the wavefield to space, where it applies a residual phase shift at each (ω, x, y). The magnitude of the phase shift depends on the difference between the actual velocity at (x, y) and the constant reference velocity used to perform the downward continuation. It completes the split-step extrapolation from z to Δz by Fourier transforming the perturbed wavefield back to wavenumber again. Split-step migration requires at most two (one forward and one inverse) spatial Fourier transforms of the wavefield at each depth; this represents a significant efficiency improvement over PSPI. In typical depth migration applications, where the migration velocity is not known with precision, this method represents a reasonable compromise between speed and accuracy, with fair ability to image steep dips. Split-step migration is an example of a screen method (De Hoop et al., 1999). These have been used since the 1970s to describe the behavior of sound waves in the ocean and electromagnetic waves in the atmosphere.

We end this section by describing a family of migration methods that promise to be very useful for 3-D prestack migration of marine streamer data. Even if the streamer is feathered, the azimuth and offset between any given source array and hydrophone in a marine streamer survey often remain relatively constant as the boat moves along, allowing us to sort marine streamer data into constant-azimuth constant-offset volumes. If the velocity is also laterally invariant, then for each volume the whole problem becomes laterally invariant, making it possible to perform the required migration convolutions efficiently in the wavenumber domain (Etgen, 1998).

Dubrulle (1983) first pointed out that Gazdag's $v(z)$ phase-shift migration, originally described for zero-offset wavefields, can be extended to operate on individual common-offset sections, even though such sections are not themselves wavefields. Ekren and Ursin (1999) later showed how Dubrulle's algorithm, simplified, becomes an efficient 2-D $v(t)$ prestack common-offset time-migration method. Dai and Marcoux (1999) then extended the method to 3-D time migration of constant-offset, constant-azimuth volumes. Their method also allows for a laterally varying imaging-velocity field by applying the procedure multiple times nonrecursively at each time level, using a number of different constant velocities. After inverse Fourier transformation, the imaging velocity at each (x, y, t) location then guides an interpolation between the computed constant-velocity images, producing a single output time-migrated image for that time level. This method is analogous to PSPI but, unlike PSPI time migration, it is not recursive. The several spatial Fourier transforms to be performed at each output migrated time level do not depend on the Fourier transforms performed at previous time levels. The cost of this method is several times the cost of a single phase-shift migration of a common-offset, common-azimuth volume. Figure 15 shows a 2-D migrated impulse calculated using this method.

Migration amplitudes

One general aspect of migration deserves mention, namely its ability to preserve the amplitudes of reflection coefficients, to be used in subsequent amplitude-variation-with-offset (AVO) analysis. This ability is common to all migration methods to some degree, and its use is becoming more widespread. Clearly, if we handle amplitudes incorrectly in any processing step, our ability to interpret the amplitudes emerging from the final step will be compromised. It is therefore important to apply migration very carefully in order to preserve amplitudes, and to pay close attention to amplitude preservation in the processing steps leading up to and following migration as well. A large theoretical and practical effort has been invested in producing amplitude-preserving migration

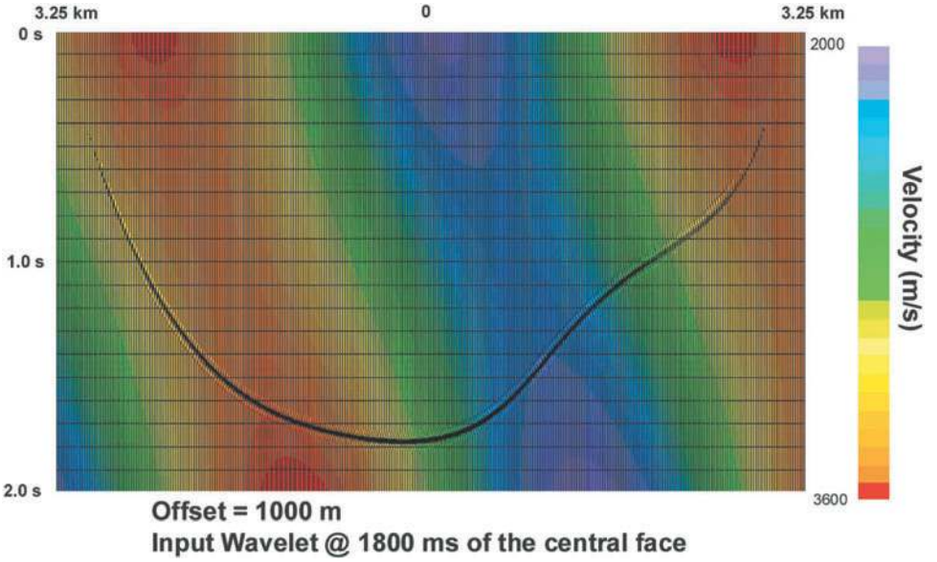

FIG. 15. An impulse migrated using a common-offset phase-shift migration that allows lateral velocity variations. This migration operator is kinematically identical to a Kirchhoff time-migration operator. For constant velocity, the impulse response would be an ellipse with foci at ± 0.5 km. The low-velocity zone (blue) causes a pronounced deviation from that shape. (From Dai and Marcoux, 1999, courtesy of Veritas DGC.)

algorithms and processing flows (e.g., Mosher et al., 1996; Gray, 1997). If we wish to follow through on the promise of determining rock and fluid properties from seismic data, or hope to use migration amplitudes as another source of "ground truth" in the management and development of reservoirs, it will become even more important to continue to assess and improve the accuracy of the amplitude treatment in our seismic migration methods.

To date, "true-amplitude" migration (or migration/inversion) has been applied successfully only in areas with a relatively simple background velocity model (see, e.g., Sollid, 2000). In complicated areas, it is unknown whether any migration method is faithful enough in obeying all the laws of seismic wave propagation to provide trustworthy amplitude behavior. This fact does not permit us to ignore amplitudes when we apply migration to complicated areas. In such areas, although we might not benefit directly by paying careful attention to amplitudes, by ignoring them we run the risk of introducing subtle artifacts into our image that are capable of causing misinterpreted structure.

VELOCITY ESTIMATION

Migration needs velocity. In order to place a reflection event that arrived at time t on a seismic record at a particular subsurface location, migration must somehow use velocity, relating the time to the distance. We never know the velocity perfectly below a few tens of meters beneath the earth's surface or more than a few meters away from a wellbore inside the earth, so we rely on estimates for the velocities inside the earth. Estimating velocities for migration ranges from trivially easy in the simplest geologic settings to extremely difficult in complex geologic structures. Correspondingly, the tools used to estimate velocities range from very simple to very complicated. Here, we discuss some velocity estimation tools that are derived from migration itself.

As we already described, time migration does not need a geological model of velocity in the earth. Instead, an imaging velocity used in time migration, which is completely analogous to the velocity used to stack traces in an unmigrated CMP gather, can be regarded as a kind of average of the interval velocities inside an inverted cone spreading upwards from an image location to encompass the migration aperture. The physics that describes this averaging is complicated in areas of dip and lateral velocity variation, making it dangerous to call time-migration imaging velocities rms velocities (as we customarily do). Doing so does allow us to use simple stacking-velocity-analysis tools to estimate interval velocities, however.

Two such tools are stacking semblance analysis, used to find the velocity that optimally stacks migrated traces in a migrated common-depth-point (CDP) gather, and stack panels, which allow a processor to pick a velocity at a location that focuses the migrated stack better than any other velocity. One migration method particularly well suited for both of these velocity-analysis tools is due to Gardner et al. (1986) and Forel and Gardner (1988). This Kirchhoff variant arranges the migration operations to output CDP gathers without an NMO correction; in other words, it requires velocity awareness only in the final step. One can then pick imaging velocities at any migrated location using stacking semblance analysis. Alternatively, one might choose to stack all the migrated gathers using a suite of different functions at each location (say, percentages of a particular function) and analyze the stack panels.

For depth migration, velocity analysis is inherently much more complicated than it is for time migration. Fortunately, if our goal is simply to produce an image, we can always use residual moveout and stack to improve the final depth-migrated result. In this way, prestack depth migration can produce images that are comparable in quality to prestack time-migrated images, even when the interval velocities are not well determined. The depth-migration interval-velocity model should not contain more structural detail than the quality of the velocity analysis supports, however. Even after residual moveout and stack, spurious structure in the velocity model will generate false structure in the depth-migrated image. This is a pitfall that time migration avoids, but only because it makes no attempt to include structural information in the migration process in the first place.

To reap the full benefits of depth migration and its ability to position events in their true spatial locations, we have to expend some effort on constructing a good interval-velocity model (Versteeg, 1994). After prestack depth migration with an incorrect velocity model, residual moveout at a particular subsurface location is due to velocity errors somewhere above the image location. Some velocity-estimation methods assume that the velocity error is restricted to the vertical column directly above the analysis point. This is clearly an oversimplification, but methods that make this assumption are widely used and are very effective in the absence of dip, structural complexity, or significant lateral velocity variation.

Traveltime tomography (Bishop et al., 1985; Stork, 1992) attempts to project the offset-dependent residual moveout along raypaths joining the subsurface location and the source and receiver locations. Tomography takes velocity estimation a significant step beyond the simpler methods based on updating the velocities vertically, but introduces complications of its own. Back projecting residual information, in time or depth, from a single location into its associated ray cone (see Figure 16), and then repeating that operation for many analysis locations, creates a potentially enormous set of equations to solve. Even after some fairly unrestrictive simplifying assumptions are applied (such as raypaths not changing even as the velocity changes), the resulting algebraic inverse problem remains daunting. The system of equations to be solved for the velocity updates, though sparse, is enormous in three dimensions, and often is overdetermined and underdetermined at the same time. The overdetermination comes from the fact that many cells of the interval velocity model are traversed by several raypaths carrying possibly conflicting information about residual moveout. The underdetermination comes from the fundamental ambiguity in deciding whether to ascribe traveltime differences along raypaths to a difference in velocity or depth.

Understanding the velocity/depth ambiguity much better than we did a decade ago, we now understand why we have problems estimating interval velocities with average errors less than 5%. To make this problem even worse, we now also recognize that velocity anisotropy is often a cause for velocity errors that are 10% and more (Banik, 1984). Anisotropy, the dependence of velocity at a particular location with propagation direction, further complicates the velocity estimation problem, particularly for depth migration. Even assuming a

simplified form of anisotropy, namely weak transverse isotropy (Thomsen, 1986), we are still left with a much larger estimation problem than before, in the sense that we must estimate three "velocity" fields and possibly one or two fields of angles that define the anisotropic symmetry axes.

On the other hand, we often have physical measurements to guide our estimation; that is, we can often use our knowledge of the properties of the rocks being imaged to estimate the anisotropic parameters. Thus, we are gaining a toehold in estimating anisotropic velocities and, although the problem is usually significantly more difficult than that of estimating isotropic velocities, it is not quite as impossible as we suspected a few years ago. For example, given a knowledge of the rocks in the anisotropic thrust sheet in Figure 4, we can estimate the sheet's anisotropy parameters to within a few percent, essentially reducing the error in imaging the structure to our uncertainty in estimating the sheet's velocity in only one direction. In this case, the velocity estimation problem including anisotropy is not significantly harder than the isotropic problem.

THE FUTURE—STUCK ON KIRCHHOFF MIGRATION?

If one migration method generates controversy among geophysicists, surely that method is Kirchhoff migration. Some geophysicists love Kirchhoff migration, because they can tell it what to do and they know how it will respond to their commands. If they want to see steep dips imaged, they increase the migration aperture. If they want greater accuracy, they use a more accurate traveltime solver. If they want to do parameter testing or an intensive migration effort on a subset of the entire survey, they get windowed output at a greatly reduced cost. No other migration method can promise this overall flexibility.

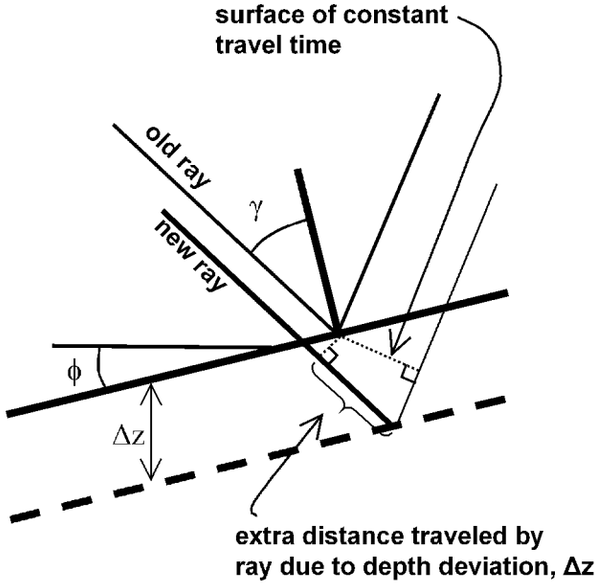

FIG. 16. Ray diagram for seismic reflection tomography, showing how changing the traveltime along two rays moves their specular reflection point. Traveltime is the integral of slowness along the raypath, so the velocity values along an entire raypath joining the source and receiver with an image point influence the image. When all source and receiver locations are considered, we see that the velocity values inside a cone joining the image point with the recording surface can influence the image. (From Stork, 1992.)

Other geophysicists hate Kirchhoff migration. No matter how many traveltime branches are included, no matter what amplitude function is used, it never seems to be as accurate as other methods can be. [There is not complete agreement even on the last statement, though. See Operto et al. (2000) for a demonstration of the imaging improvement possible if we use all the traveltime branches]. Indeed, while all migration methods make some approximations, Kirchhoff migration relies more heavily than any of the others on approximations involving high-frequency asymptotics. Kirchhoff migration consequently restricts seismic energy travelpaths to at most a few raypaths between image locations and source or receiver locations. Real band-limited wavepaths are considerably more complicated than this (Woodward, 1992).

Is one camp or the other completely right? Is Kirchhoff migration the best method or the worst method? Given the current state of the seismic data processing industry, with the size of our imaging problems growing at about the same rate as computing capacity, we can't envision the disappearance of Kirchhoff migration and all its variants such as Gaussian beam migration for some time. Its flexibility is just too great to give it up in favor of methods that promise somewhat greater accuracy given very precise knowledge of velocity. If our record in estimating velocity were much better than it has been in the past, there might be cause for dismissing Kirchhoff migration as a tool for the second millennium. In fact, velocity estimation remains a fundamental imaging problem, especially given our relatively recent awareness of anisotropic effects. Kirchhoff-migrated images are usually as useful as, and much cheaper to obtain than, images from competing methods when velocity uncertainty remains on the order of 5% or more.

On the other hand, there are imaging problems for which Kirchhoff migration is simply not good enough. Although it is true that, given incorrect velocities, no migration method will produce images good enough to map the detailed structure and stratigraphy of subsalt fault blocks, for example, it is also true that standard implementations of Kirchhoff migration simply cannot produce good images in such cases even given perfect velocities.

Recent advances in marine acquisition technology have demonstrated that this issue is of more than academic interest. To date, 3-D marine surveys acquired with towed streamers have been prestack migrated almost exclusively using Kirchhoff techniques. This is because the wavefield continuation methods are forced to pad outside the actual recording spread, as already described. In this case, the pad consists of extra zero traces placed at the end of the streamers to accommodate the in-line migration aperture, plus several extra streamers with zero traces to accommodate the cross-line migration aperture. The computational penalty of migrating all these (initially zero) extra traces is enormous.

Fixed-cable acquisition permits wavefield-continuation methods to avoid this penalty completely, giving hope for the routine use of non-Kirchhoff imaging methods for a large number of marine surveys. Instead, we can migrate common-receiver records, where the wavefield observed at any one of the fixed receivers on (or tethered above) the bottom is sampled by a spread of source locations. This wavefield is usually well sampled and contains enough source locations to eliminate

the need for padding with zero traces. Performing common-receiver migration on these 3-D records using extremely accurate wavefield-continuation methods is already feasible today and might be commonplace within a few years (Krail, 1994; Wyatt et al., 2000). Figure 17 compares subsalt-migrated depth slices from a synthetic 3-D model using Kirchhoff and wavefield migration (O'Brien and Etgen, 1998); wavefield migration has imaged all the reflectors much more clearly than Kirchhoff migration has.

A second way around the problem is to build new 3-D algorithms that are better suited to migrating data from towed streamers. Biondi and Palacharla (1996) have made one of the first major steps in this direction, presenting a fairly efficient 3-D migration scheme designed for data acquired along a single azimuth. This 3-D depth migration is an approximate wavefield-continuation method that maintains the original (multiple 2-D line) geometry as it downward continues the data. It uses as its kernel several 2-D applications of any migration method that is more accurate than Kirchhoff migration. The single-azimuth data needed for this migration scheme can be obtained by performing an azimuth-moveout (AMO) transform (Biondi et al., 1998) on the towed streamer data (even when there are fairly large azimuthal variations from the near to far offsets because of multiple-cable acquisition).

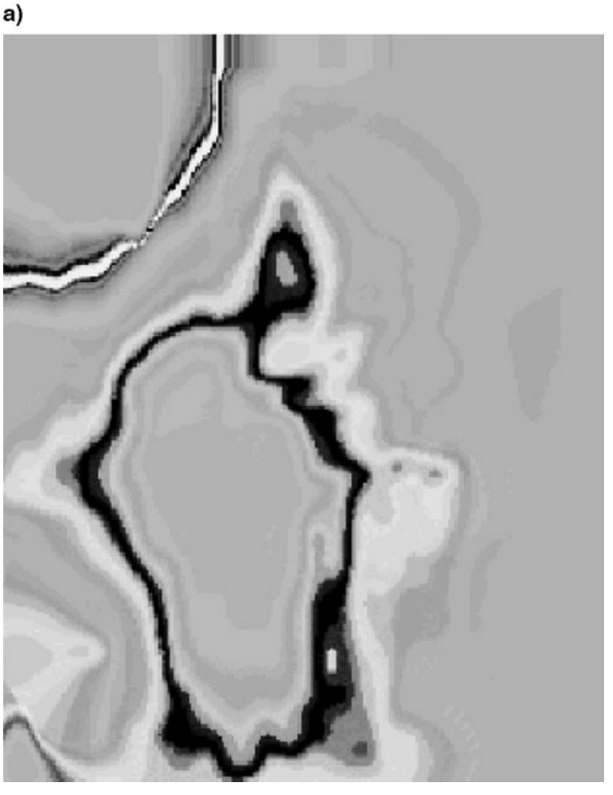

FIG. 17. (a) Depth slice (4500 m) from a 3-D synthetic F-D model showing subsalt reflectors. (b) Common-receiver wavefield-migrated depth slice at 4500 m showing correctly imaged reflectivity. (c) Common-receiver Kirchhoff-migrated depth slice at 4500 m showing much less clarity in the subsalt image than the wavefield-migrated image. (From O'Brien and Etgen, 1998.)

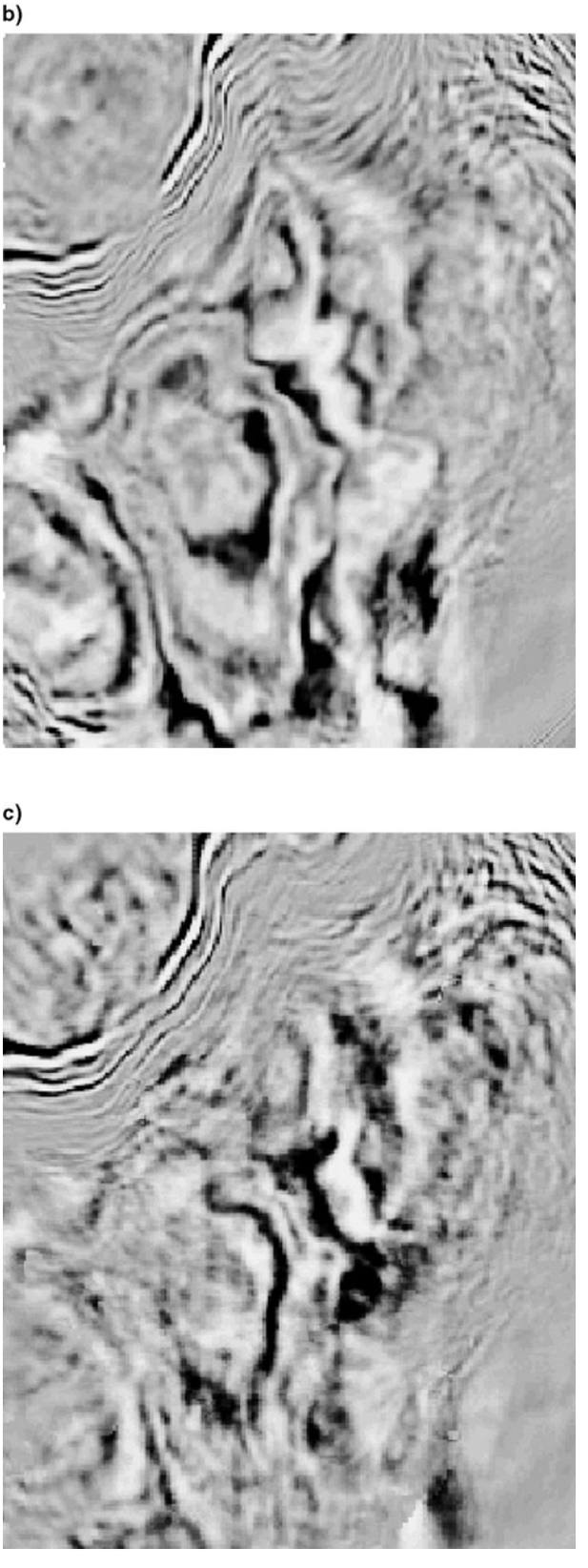

FIG. 17. (Continued).

These methods make approximations that might compromise their accuracy and they are still in early testing, but first results have been encouraging (Figure 18). If methods such as this prove successful, then geophysicists will have a range of choices for 3-D prestack migration of towed streamer data and will be able to choose a method for a given data set based on merit, not just economics.

CONCLUSIONS: THE NEAR-TERM FUTURE OF IMAGING

For many years migration was the culminating step of the seismic processing flow, feeding directly into maps of structure and stratigraphy. Nowadays, migration is much more likely to be an intermediate step, feeding information into other seismic processes. Migrated amplitudes are used for AVO analysis and for other forms of seismic attribute analysis. Migrated structural information is used in coherency analysis to delineate small-scale as well as large-scale structure. The velocities obtained from prestack depth migration are used not only to check the plausibility of the underlying geologic model, but also to estimate quantities such as pore pressure in the subsurface.

Perhaps the most-recognized application of migration is for applying interpretational knowledge and skills during the velocity-estimation process. Gradually over the past decade, with the progression from poststack time migration to prestack depth migration, building velocity models has increasingly become a task for people with geologic knowledge to accompany their processing skills—interpreters, in a word. Although initial velocity model-building packages were relatively clumsy, and present-day packages combining velocity estimation, model building, and visualization still leave much to be desired, significant progress in speeding up the process of iterative prestack depth migration has occurred in the past few years. In the near future, velocity model-building tools will allow interpreters to update velocity models interactively while viewing the effects of the updates on the migrated gathers or even the migrated stacks. Interactive workstation technology has enabled this already to some degree (Murphy and Gray, 1999), and increased communications bandwidth, visualization capability, and computational speed will complete the task.

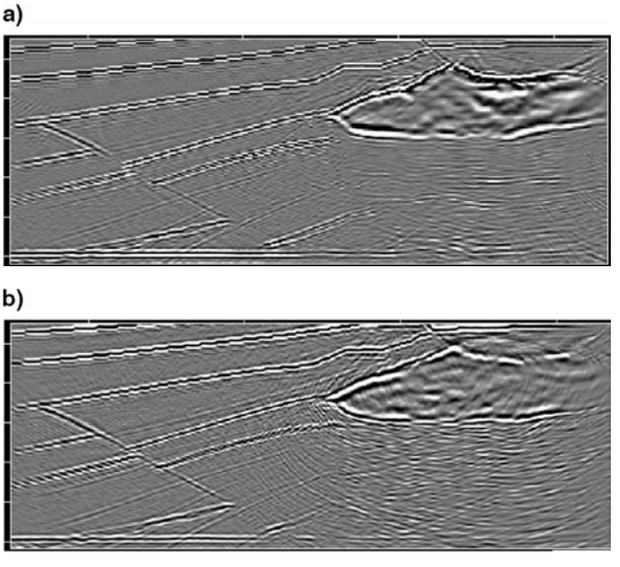

FIG. 18. (a) Wavefield-migrated profile from the SEG/EAGE salt model. (b) The same profile migrated using Kirchhoff migration. Wavefield migration has produced a cleaner, more correct image. (From Biondi and Vaillant, 2000.)

Migration has a greater amount of interaction with earlier steps as well. Today, most seismic acquisition programs are designed to include an appropriate aperture and spatial sampling for migration. In processing, enhancing the signal for migration has always been paramount, but now some processes are being used to enhance what used to be considered noise (e.g., multiples or converted-wave events) so that they can also be migrated.

Converted-wave events are part of a larger wavefield than has been routinely used for migration, namely the elastic wavefield. Mathematically, the acoustic wave equation describes the propagation of compressional waves (P-waves) in fluids (e.g., sound waves in air or water). All the migration methods described in this paper have assumed acoustic wave propagation, and this approximation is usually adequate if our goal is to image P-waves in sedimentary basins. In reality, most of the earth's subsurface is solid, and so the elastic wave equation provides a more physically meaningful model of what happens in seismic experiments. In some exploration environments, making an effort to treat elastic propagation effects as signal instead of noise can be worthwhile. Two such instances are (1) propagation through relatively large bodies of weakly gas-charged sediments ("gas clouds"), which tends to scatter and attenuate P-waves in favor of energy propagating in a converted mode, and (2) propagation in structurally complex settings, where the P-wave critical angle is easily encountered and mode conversion accounts for a large portion of the recorded seismic energy.

Situations such as these are not commonplace, but they are increasing, and they require processing (including migration) that accounts for mode conversions when they occur. If the mode conversion takes place at reflection, converting incident P-waves to reflected shear waves (so-called "C-waves"), it is kinematically straightforward to perform prestack migration: one merely uses P-wave velocities for the source wavefields, and shear-wave velocities for the receiver wavefields (e.g., for Kirchhoff migration, we would use P-wave velocities when calculating source to image point traveltimes, but shear-wave velocities when calculating image point to receiver traveltimes). This kinematic approximation is the basis for current techniques for migrating converted-wave data, even though it ignores the true complexities of elastic-wave propagation in a 3-D heterogeneous earth. Also, in cases where mode conversion can occur anywhere along the propagation path, not just at reflection, the problem is much harder. It requires a solution that somehow allows for full elastic downward continuation and imaging, such as reverse-time migration (Chang and McMechan, 1994).

Along with an increased use of converted-wave and full elastic migration comes an increase in the use of anisotropy, not only as an extra velocity parameter but also for determining the orientation of fractures in the rocks being imaged. At present, our ability to estimate fracture orientation is very limited, but the need for reliable placement of directional wells that exploit our knowledge of fracture systems requires us to incorporate this knowledge in, or derive the knowledge from, our imaging methods.

These few developments do not, by any means, represent all the advances that will be made to our knowledge and practice of seismic migration in the next few years. Nor do they begin to scratch the surface of what might take place in the decades ahead. Since the early days of mechanical migration, geophysicists have continued to innovate in bringing forward the science and the technology of imaging the earth's interior in the search for hydrocarbons. These scientists and engineers have borrowed freely from, and donated willingly to, the general store of technical knowledge (medical, electromagnetic, atmospheric, oceanic, and scattering, to name a few) in advancing the state of seismic imaging. They have also faced economic hurdles over the past decade and more that have added an extra burden to the technical task of discovering ever more elusive hydrocarbon traps. Still, they continue to rise to the theoretical and practical challenges of producing accurate, efficient seismic imaging solutions.

ACKNOWLEDGMENTS

We thank Sven Treitel for suggesting this project and for his patience in awaiting its outcome. We also thank many colleagues who contributed their time and material, especially Biondo Biondi, Ross Hill, and Sverre Brandsberg-Dahl. Finally, we thank Placer Deguzman for assembling all the pieces into a single document.

REFERENCES

Abma, R., Sun, J., and Bernitsas, N., 1999, Antialiasing methods in Kirchhoff migration: Geophysics, **64**, 1783–1792.
Aminzadeh, F., Burkhard, N., Nicoletis, L., Rocca, F., and Wyatt, K., 1994, SEG/EAEG 3-D modeling project: 2nd update: The Leading Edge, **13**, 949–952.
Audebert, F., Nichols, D., Rekdal, T., Biondi, B., Lumley, D. E., and Urdaneta, H., 1997, Imaging complex geologic structure with single-arrival Kirchhoff prestack depth migration: Geophysics, **62**, 1533–1543.
Banik, N. C., 1984, Velocity anisotropy of shales and depth estimation in the North Sea basin: Geophysics, **49**, 1411–1419.
Baysal, E., Kosloff, D. D., and Sherwood, J. W. C., 1983, Reverse time migration: Geophysics, **48**, 1514–1524.
Berkhout, A. J., 1984, Seismic migration: Imaging of acoustic energy by wavefield extrapolation. B: Practical aspects, Elsevier Science Publ.
Berryhill, J. R., 1984, Wave equation datuming before stack (short note): Geophysics, **49**, 2064–2067.
Bevc, D., 1997, Imaging complex structures with semirecursive Kirchhoff migration: Geophysics, **62**, 577–588.
Biondi, B., Fomel, S., and Chemingui, N., 1998, Azimuth moveout for 3-D prestack imaging: Geophysics, **63**, 574–588.
Biondi, B., and Palacharla, G., 1996, 3-D prestack migration of common-azimuth data: Geophysics, **61**, 1822–1832.
Biondi, B., and Vaillant, L., 2000, 3-D wave-equation prestack imaging under salt: 70th Ann. Internat. Mtg., Soc. Expl. Geophys., Expanded Abstracts, 906–909.
Bishop, T. N., Bube, K. P., Cutler, R. T., Langan, R. T., Love, P. L., Resnick, J. R., Shuey, R. T., Spindler, D. A., and Wyld, H. W., 1985, Tomographic determination of velocity and depth in laterally varying media: Geophysics, **50**, 903–923.
Bleistein, N., 1987, On the imaging of reflectors in the earth: Geophysics, **52**, 931–942.
Chang, W., and McMechan, G. A., 1994, 3-D elastic prestack, reverse-time depth migration: Geophysics, **59**, 597–610.
Claerbout, J. F., 1985, Imaging the earth's interior: Blackwell Scientific Publications, Inc.
Claerbout, J. F., and Doherty, S. M., 1972, Downward continuation of moveout-corrected seismograms: Geophysics, **37**, 741–768.
Dai, N., and Marcoux, M. O., 1999, Constant-offset–constant-azimuth *f-k* migration for $v(z)$: 69th Annual Internat. Mtg., Soc. Expl. Geophys., Expanded Abstracts, 1114–1117.
De Hoop, M. V., Le Rousseau, J. H., and Wu, R.-S., 2000, Generalization of the phase-screen approximation for the scattering of acoustic waves: Wave Motion, **31**, 43–70.
Dix, C. H., 1955, Seismic velocities from surface measurements: Geophysics, **20**, 68–86.
Docherty, P., 1991, A brief comparison of some Kirchhoff integral formulas for migration and inversion: Geophysics, **56**, 1164–1169.
Dubrulle, A. A., 1983, Numerical methods for the migration of constant-offset sections in homogeneous and horizontally-layered media: Geophysics, **48**, 1195–1203.
Ehinger, A., Lailly, P., and Marfurt, K. J., 1996, Green's function implementation of common-offset wave-equation migration: Geophysics, **61**, 1813–1821.
Ekren, B. O., and Ursin, B., 1999, True-amplitude frequency-wavenumber constant-offset migration: Geophysics, **64**, 915–924.
Etgen, J. T., 1994, Stability of explicit depth extrapolation through laterally-varying media: 64th Annual Internat. Mtg., Soc. Expl. Geophys., Expanded Abstracts, 1266–1269.
——— 1998, $V(z)$ *F-K* prestack migration of common-offset common-azimuth data volumes, part 1: theory: 68th Annual Internat. Mtg., Soc. Expl. Geophys., Expanded Abstracts, 1835–1838.
Etgen, J., and Nichols, D., 1999, Application of the Li correction to explicit depth-extrapolation methods: 69th Annual Internat. Mtg., Soc. Expl. Geophys., Expanded Abstracts, 1366–1369.
Fei, T., Dellinger, J. A., Murphy, G. E., Hensley, J. L., and Gray, S. H., 1998, Anisotropic true-amplitude migration: 68th Annual Internat. Mtg., Soc. Expl. Geophys., Expanded Abstracts, 1677–1679.
Forel, D., and Gardner, G. H. F., 1988, A three-dimensional perspective on two-dimensional dip moveout: Geophysics, **53**, 604–610.
Gardner, G. H. F., Ed., 1985, Migration of seismic data: Soc. Expl. Geophys.
Gardner, G. H. F., Wang, S. Y., Pan, N. D., and Zhang, Z., 1986, Dip moveout and prestack imaging: 18th Offshore Tech. Conf., **2**, 75–84.
Gazdag, J., 1978, Wave equation migration with the phase-shift method: Geophysics, **43**, 1342–1351.
Gazdag, J., and Sguazzero, P., 1984, Migration of seismic data by phase shift plus interpolation: Geophysics, **49**, 124–131.
Gray, S. H., 1992, Frequency-selective design of the Kirchhoff migration operator: Geophys. Prosp., **40**, 565–571.
——— 1997, True-amplitude seismic migration: A comparison of three approaches: Geophysics, **62**, 929–936.
Gray, S. H., and May, W. P., 1994, Kirchhoff migration using eikonal equation traveltimes: Geophysics, **59**, 810–817.
Hale, D., 1984, Dip-moveout by Fourier transform: Geophysics, **49**, 741–757.
Hale, D., 1991a, Stable explicit depth extrapolation of seismic wavefields: Geophysics, **56**, 1770–1777.
——— 1991b, 3-D depth migration by McClellan transformations: Geophysics, **56**, 1778–1785.
Hale, D., Hill, N. R., and Stefani, J., 1992, Imaging salt with turning seismic waves: Geophysics, **57**, 1453–1462.
Hill, N. R., 1990, Gaussian beam migration: Geophysics, **55**, 1416–1428.
——— 2001, Prestack Gaussian-beam depth migration: Geophysics, **66**, 1240–1250.
Holberg, O., 1988, Towards optimum one-way wave propagation: Geophys. Prosp., **36**, 99–114.
Judson, D. R., Schultz, P. S., and Sherwood, J. W. C., 1978, Equalizing the stacking velocities of dipping events via Devilish: Presented at the 48th Ann. Internat. Mtg., Soc. Expl. Geophys. (Brochure published by Digicon Geophysical Corp.)
Kelly, K. R., Ward, R. W., Treitel, S., and Alford, R. M., 1976, Synthetic seismograms—A finite-difference approach: Geophysics, **41**, 2–27.
Krail, P. M., 1994, Vertical cable as a subsalt imaging tool: The Leading Edge, **13**, 885–887.
Larner, K. L., Hatton, L., Gibson, B. S., and Hsu, I-C., 1981, Depth migration of imaged time sections: Geophysics, **46**, 734–750.
Leslie, J. M., and Lawton, D. C., 1998, Depth migration of anisotropic physical model data: Geo-Triad 1998 Abstracts, 77–78.
Li, Z., 1991, Compensating finite-difference errors in 3-D migration and modeling: Geophysics, **56**, 1650–1660.
Loewenthal, D., Lu, L., Roberson, R., and Sherwood, J., 1976, The wave equation applied to migration: Geophys. Prosp., **24**, 380–399.
Lumley, D., Claerbout, J., and Bevc, D., 1994, Anti-aliased Kirchhoff 3-D migration: 64th Ann. Internat. Mtg., Soc. Expl. Geophys., Expanded Abstracts, 1282–1285.
Mayne, W. H., 1962, Common reflection point horizontal data stacking techniques: Geophysics, **27**, 927–938.
McMechan, G. A., 1983, Migration by extrapolation of time-dependent boundary values: Geophys. Prosp., **31**, 413–420.
Miller, D., Oristaglio, M., and Beylkin, G., 1987, A new slant on seismic imaging: Migration and integral geometry: Geophysics, **52**, 943–964.
Mosher, C. C., Keho, T. H., Weglein, A. B., and Foster, D. J., 1996, The impact of migration on AVO: Geophysics, **61**, 1603–1615.

Murphy, G. E., and Gray, S. H., 1999, Manual seismic reflection tomography: Geophysics, **64**, 1546–1552.
Nolan, C. J., and Symes, W., 1996, Imaging and coherency in complex structures: 66th Ann. Mtg., Soc. Expl. Geophys., Expanded Abstracts, 359–362.
O'Brien, M. J., and Etgen, J. T., 1998, Wavefield imaging of complex structures with sparse, point-receiver data: 68th Ann. Mtg., Soc. Expl. Geophys., Expanded Abstracts, 1365–1368.
Operto, M. S., Xu, S., and Lambaré, G., 2000, Can we quantitatively image complex structures with rays?: Geophysics, **65**, 1223–1238.
Santos, L., Schleicher, J., Tygel, M., and Tygel, M., 2000, Seismic modeling by demigration: Geophysics, **65**, 1281–1289.
Schneider, W. A., 1971, Developments in seismic data processing and analysis (1968–1970): Geophysics, **36**, 1043–1073.
———1978, Integral formulation for migration in two and three dimensions: Geophysics, **43**, 49–76.
Sollid, A., 2000, Imaging of ocean-bottom seismic data: Ph.D. thesis, Norwegian Univ. of Science and Technology.
Stoffa, P. L., Fokkema, J. T., de Luna Freire, R. M., and Kessinger, W. P., 1990, Split-step Fourier migration: Geophysics, **55**, 410–421.
Stolt, R. H., 1978, Migration by Fourier transform: Geophysics, **43**, 23–48.
Stork, C., 1992, Reflection tomography in the postmigrated domain: Geophysics, **57**, 680–692.
Thomsen, L., 1986, Weak elastic anisotropy: Geophysics, **51**, 1954–1966.
Versteeg, R., 1994, The Marmousi experience: Velocity model determination on a synthetic complex data set: The Leading Edge, **13**, 927–936.
Versteeg, R., and Grau, G., Eds., 1991, The Marmousi experience: Proceedings of the 1990 EAEG Workshop, 52nd EAEG Meeting, Eur. Assoc. Expl. Geophys.
Vidale, J., 1988, Finite-difference calculation of traveltimes: Bull. Seis. Soc. Am., **78**, 2062–2076.
Whitmore, N. D., 1983, Iterative depth migration by backward time propagation: 53rd Ann. Internat. Mtg., Soc. Expl. Geophys., Expanded Abstracts, 382–385.
Whitmore, N. D., Gray, S. H., and Gersztenkorn, A., 1988, Two-dimensional poststack depth migration: A survey of methods: First Break, **6**, 189–197.
Woodward, M. J., 1992, Wave-equation tomography: Geophysics, **57**, 15–26.
Wyatt, K. D., DeSantis, J. E., Valasek, P. A., Chen, T. C., Shen, Y., Meng, Z., Branham, K. L., Liu, W., Fromr, E., and Delome, H., 2000, A 3-D wavefield imaging experiment in the deepwater Gulf of Mexico: 70th Ann. Internat. Mtg., Soc. Expl. Geophys., Expanded Abstracts, 854–857.
Yilmaz, Ö., 1979, Pre-stack partial migration: Ph.D. thesis, Stanford University.
———1987, Seismic data processing: Soc. of Expl. Geophys.
Young, K.-T., Meng, X., Montecchi, P., and Notfors, C., 1999, Subsalt imaging in Walker Ridge, Gulf of Mexico: 69th Ann. Internat. Mtg., Soc. Expl. Geophys., Expanded Abstracts, 1099–1102.